



Contents lists available at ScienceDirect

Journal of Nuclear Materials

journal homepage: www.elsevier.com/locate/jnucmat

Deuterium trapping in tungsten damaged by high-energy hydrogen ion irradiation

M. Fukumoto^{a,*}, H. Kashiwagi^a, Y. Ohtsuka^a, Y. Ueda^a, M. Taniguchi^b, T. Inoue^b, K. Sakamoto^b, J. Yagyu^b, T. Arai^b, I. Takagi^c, T. Kawamura^d^a Graduate School of Engineering, Osaka University, 2-1 Yamadaoka, Suita, Osaka 565-0871, Japan^b Japan Atomic Energy Agency, 801-1 Mukoyama, Naka, Ibaraki 311-0193, Japan^c Department of Nuclear Engineering, Kyoto University, Yoshida, Sakyo-ku, Koto 606-8501, Japan^d Interdisciplinary Graduate School of Engineering Science, Kyushu University, 6-1 Kasugakoen, Kasuga-shi, Fukuoka 816-8580, Japan

ARTICLE INFO

PACS:
28.52.Fa
52.40.Hf
61.80.Jh
79.20.Rf
61.82.Bg

ABSTRACT

Effects of radiation damage on deuterium trapping in tungsten were investigated using SIMS/NRA and TDS techniques. Radiation damage of ~ 4.8 dpa was produced by 300 and 700 keV hydrogen ions, then deuterium ions were implanted at 473 K to fluences of $0.5\text{--}8.0 \times 10^{24}$ D⁺/m². Deuterium concentration at ~ 0.1 μm in depth was saturated at the lowest fluence ($\sim 5.0 \times 10^{23}$ D⁺/m²), while the D retention at ~ 1.0 μm deep was not saturated at the highest fluence of $\sim 8.0 \times 10^{24}$ D⁺/m². On the other hand, deuterium behavior simulated by the TMAP7 code showed that the defects were filled with the implanted D from the top surface and all of the traps were filled at the fluence of $\sim 7.5 \times 10^{22}$ D⁺/m², which was much lower than the fluences in this experiment. TDS spectra suggested that the implanted D was trapped at the radiation-induced defects which had desorption peaks at ~ 770 and ~ 920 K.

© 2009 Elsevier B.V. All rights reserved.

1. Introduction

Tungsten-based materials are candidates for next generation fusion devices. The advantages of tungsten are its natures of high melting temperature and low sputtering yield by fuel particles. In ITER, tungsten will be used at the baffle plates and the domes of diverter regions. During plasma operation, energetic tritium as well as deuterium particles impinge on and are retained in the tungsten. Extensive studies have been made on the behavior of hydrogen isotopes in various tungsten materials [1–10]. Most of the samples used in the previous studies had no radiation damage.

In DT fusion reactors, however, radiation induced defects are produced in tungsten due to the 14 MeV neutron bombardment. Therefore, it is important to study the tritium behavior such as retention, release, and diffusion, in neutron-damaged tungsten. Recently, deuterium retention and release from 800 MeV proton-irradiated and post-annealed tungsten was studied using TDS (Thermal Desorption Spectroscopy) [11]. They showed that radiation induced defects were successfully removed by annealing at 1273 K for ~ 6 h. Arkhipov et al. showed that deuterium retention in 10 keV H⁺ damaged tungsten was 27 times as high as undamaged one [12]. These studies showed only deuterium retention in damaged tungsten but deuterium depth distributions were not observed. To understand the deuterium trapping in damaged tung-

sten in more detail, it is important to measure the deuterium depth distributions.

The purpose of this work is to investigate the deuterium behavior such as retention and depth distributions in tungsten damaged by high-energy ions. Deuterium depth distributions of the damaged samples were measured with SIMS (Secondary Ion Mass Spectrometry) and NRA (Nuclear Reaction Analysis). Deuterium retention was observed by TDS. Experimental results were compared with those of the TMAP7 simulations [13].

2. Experimental

The polycrystalline W sheets, 1 mm thick and 99.99 at.% pure (A.L.M.T.Corp.), were used. These were powder metallurgy and hot rolled products. In the manufacturing process, the W sheets were annealed at 1173 K for 0.5 h in a hydrogen atmosphere to relieve internal stresses. Tungsten samples, $\sim 10 \times 10$ mm², were cut from the sheets and mechanically polished less than ~ 0.1 μm roughness.

Radiation damage was produced using a MeV accelerator MTF [14]. Negative ions of 300 and 700 keV H⁻ were used for damage creation. According to the results of Keys and Moteff [15], the Stage III recovery of neutron irradiated tungsten is promoted above 473 K. Therefore, in order to prevent recovery of produced damage, high energy H⁻ ions were irradiated repeatedly for 0.2–1.0 s every 60 s to limit the highest surface temperature below 473 K. Sample temperature during irradiation was monitored using a pyrometer.

* Corresponding author.

E-mail address: fukumoto@st.eie.eng.osaka-u.ac.jp (M. Fukumoto).

Following damage creation, D^+ implantation was performed using an ion beam irradiation device HiFIT [16]. Incident ion species were D^+ , D_2^+ , and D_3^+ with the energies of 1.0 keV. The deuterium atom species ratios irradiated to samples were 50%, 30%, and 20% for 0.3 keV, 0.5 keV, and 1.0 keV D, respectively. Typical flux densities were $\sim 1.5 \times 10^{20} D^+/m^2s$. Irradiated fluence was changed from 0.5×10^{24} to $8.0 \times 10^{24} D^+/m^2$. Although the ranges of three species are the order of nm, the diffusion length of deuterium in tungsten is more than μm . Therefore, influence of the simultaneous irradiation of three species would not affect the results. Sample temperature measured by a chromel–alumel thermocouple was kept at 473 K.

SIMS analysis was performed to measure deuterium depth profiles before TDS. SIMS analysis would not significantly affect the subsequent TDS measurement since the size of sputtered spot ($\sim 0.1 mm^2$) was much smaller than the D implanted area ($\sim 19.6 mm^2$). Temperature of the sputtering region by the primary ion beam was not monitored. NRA data was used to absolutely calibrate the secondary ion signals (D^-).

For TDS measurements, the samples were heated from 300 to 1100 K at a heating rate of $\sim 1 K/s$ and released D_2 was monitored using a quadruple mass spectrometer (QMS). The QMS signals were calibrated by a standard He leak bottle by collecting relative ionization efficiency before each TDS measurement.

3. Results and discussions

SIMS depth profiles of the one undamaged sample and two damaged samples are shown in Fig. 1(a). Distributions of DPA (Displacement Per Atom) calculated by TRIM-88 code [17] for the two different damaged samples are shown in Fig. 1(b). The deuterium depth distribution in the undamaged sample was almost constant within the observed area except for the top surface. In the case of

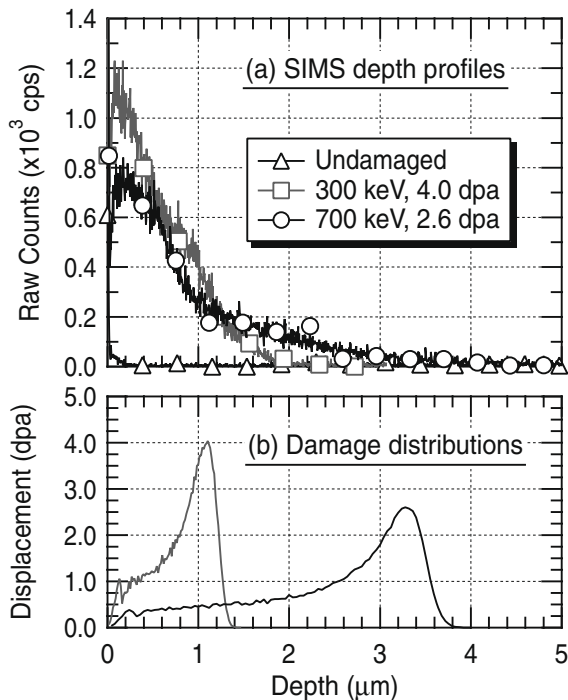


Fig. 1. (a) SIMS depth profiles for undamaged and two damaged samples irradiated with 1 keV deuterium ions to $5.0 \times 10^{23} D^+/m^2$ at 473 K. (b) Damage distributions for the 300 and 700 keV H^- damaged samples estimated by TRIM-88 code [17]. Incident H^- fluences for damage creation were $\sim 1.3 \times 10^{22}$ and $\sim 1.2 \times 10^{22} H^-/m^2$ for 300 and 700 keV H^- damaged samples, respectively.

the damaged samples, deuterium concentration was much higher than that of the undamaged sample within the damaged zone. Beyond the damaged zone, the deuterium concentration of the damaged sample was similar to that of the undamaged sample. Therefore, it can be concluded that the implanted deuterium was mainly trapped at the radiation damage produced by the high-energy H^- beam.

The fluence dependence of D distributions for the ~ 4.8 dpa damaged samples at 473 K is shown in Fig. 2. The damage distribution estimated by the TRIM code is also shown. The incident fluence for damage creation was $\sim 1.5 \times 10^{22} H^-/m^2$. For the fluence of more than $5.0 \times 10^{23} D^+/m^2$, D concentration near the sample surface ($\sim 0.1 \mu m$ in depth) became saturated with $\sim 0.9 \times 10^{27} D/m^3$. On the other hand, no saturation seemed to occur even at the fluence of $8.0 \times 10^{24} D^+/m^2$ at $\sim 1 \mu m$ in depth. If the D concentrations were equal to the trap densities at the $\sim 0.1 \mu m$ in depth, the total trap densities are estimated to be ~ 0.014 traps/W for the radiation damage ~ 1.0 dpa and the implant temperature 473 K.

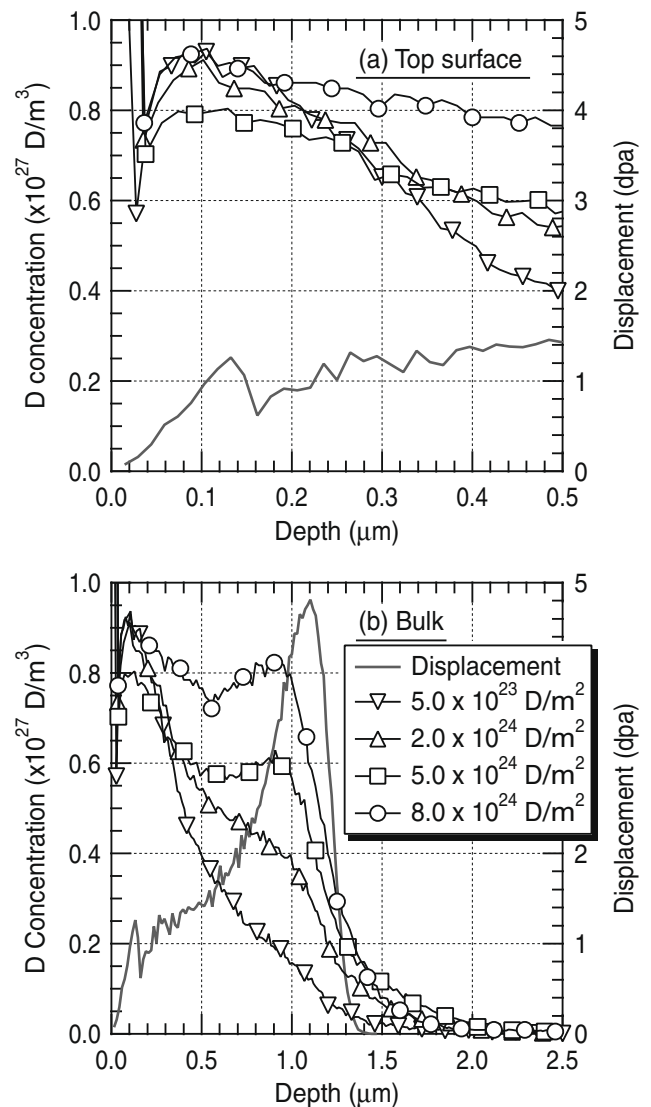


Fig. 2. SIMS depth profiles for ~ 4.8 dpa damaged samples as a function of incident fluence at (a) top surface and (b) bulk. Samples were irradiated with 1 keV deuterium ions at 473 K. The damage distribution estimated by the TRIM-88 code is also shown with right axis. Incident H^- fluence for damage creation were $\sim 1.5 \times 10^{22} H^-/m^2$.

Thermal desorption spectra were obtained for the ~ 4.8 dpa damaged samples in the fluence of $0.5\text{--}8.0 \times 10^{24}$ D^+/m^2 at 473 K. For comparison, desorption spectra of one undamaged sample irradiated to 5.0×10^{24} D^+/m^2 at 473 K was also obtained. Fig. 3 shows the TDS spectra for the ~ 4.8 dpa samples with the fluence of 5.0×10^{24} D^+/m^2 . According to the results of curve fitting of the TDS profiles by three Gaussian functions, it was found that the peak positions were ~ 770 K, ~ 860 K, and ~ 920 K (Fig. 3). In this paper, these peaks are named with Peak 1, Peak 2, and Peak 3.

The fluence dependence of D retention for the three peaks is shown in Fig. 4. For the damaged samples with the fluence of 5.0×10^{24} D^+/m^2 , the D retention in the Peak 1 was about one order of magnitude larger than that of the undamaged sample. Furthermore, the D retention in the Peak 1 was increased with the D fluences. The D retention in the Peak 2 was almost constant regardless of the fluences. The D retention in the Peak 3 was only observed from the damaged samples and was also increased with the D fluences. Therefore, it is suggested from Fig. 4 that implanted D would be trapped at the radiation induced defects which related to the desorption peaks at ~ 770 K (Peak 1) and ~ 920 K (Peak 3).

Poon et al. reported that TDS profiles obtained from single crystal tungsten irradiated at 300 K showed desorption peaks at 520 and 640 K [18]. These peaks are considered to be due to desorption of trapped D from single vacancies. The peak temperature of the Peak 1 (~ 770 K) was higher than the results obtained by Poon et al. [18]. Therefore, it can be considered that the Peak 1 would not be desorption from single vacancies. Deuterium desorption spectra of 10 keV H^+ damaged W exposed with 100 eV D plasma at 500 K was obtained by Arkhipov et al. [12]. They reported that the D desorption which positioned at 750–800 K was increased by the number of vacancy clusters formed by the 10 keV H^+ pre-irradiation. Therefore, it can be considered that the Peak 1 was attributed to desorption from vacancy clusters. The Peak 2 (~ 860 K) desorption spectra could be attributed to desorption from intrinsic defect sites in the samples since similar D retention from the damaged and undamaged samples was observed. The peak temperature of the Peak 3 (~ 920 K) was similar to that observed by Poon et al. (~ 900 K) [18] which could be due to desorption from voids. Therefore, the Peak 3 could correspond to voids.

Deuterium depth profiles for the ~ 4.8 dpa damaged samples were simulated by TMAP7, see Fig. 5. The damage distributions

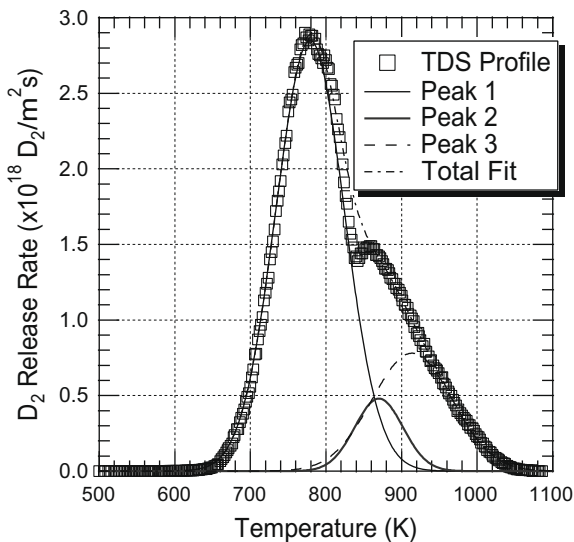


Fig. 3. TDS spectra obtained from the ~ 4.8 dpa ($\sim 1.5 \times 10^{22}$ H^-/m^2) damaged sample irradiated to 5.0×10^{24} D^+/m^2 at 473 K. Gaussian fits to determine the relative amounts of D associated with each desorption peak is also shown.

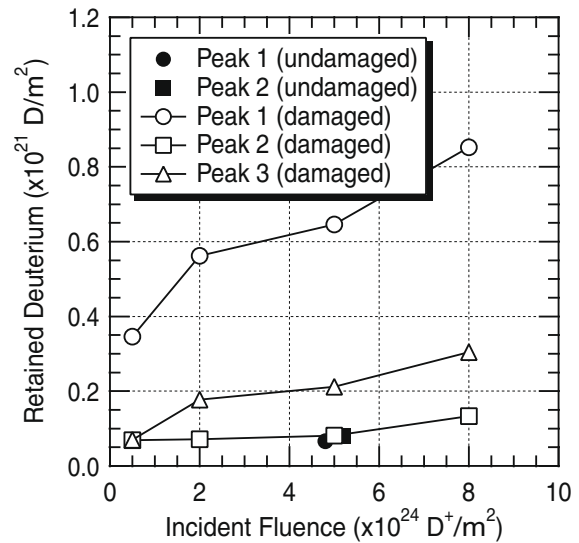


Fig. 4. D retention of each desorption peak as a function of incident fluence obtained from ~ 4.8 dpa ($\sim 1.5 \times 10^{22}$ H^-/m^2) damaged samples. All samples were irradiated with the 1 keV deuterium ions at 473 K.

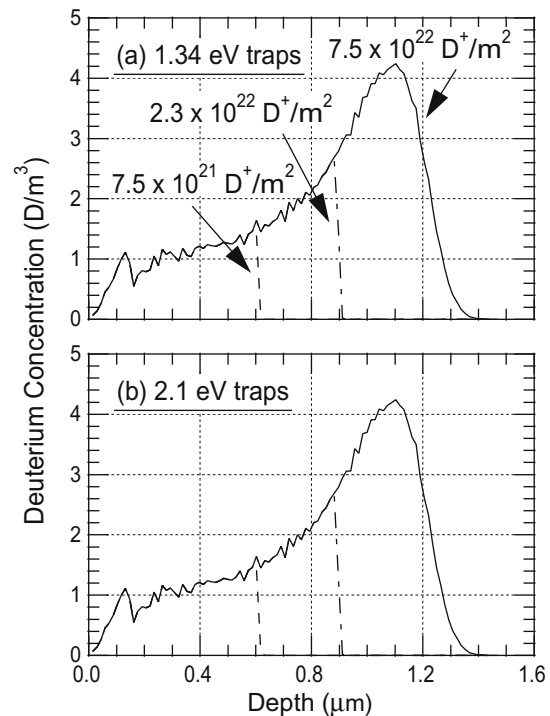


Fig. 5. D depth profiles for the ~ 4.8 dpa ($\sim 1.5 \times 10^{22}$ H^-/m^2) damaged samples simulated by TMAP7. (a) 1.34 eV trap energy and (b) 2.1 eV trap energy were assumed. The damage distributions in the samples were obtained by TRIM calculations. The damage concentration used in the TMAP7 simulations was assumed to be 0.014 traps/W.

(by the TRIM code) and trap concentrations (0.014 traps/W) in the samples were used for the TMAP7 simulations. The Fraunfelder's diffusion coefficient corrected to the deuterium one was used,

$$D = 2.9 \times 10^{-7} \exp(-0.39 \text{ eV}/kT) \text{ m}^2/\text{s}, \quad (1)$$

where k is the Boltzmann constant and T is the temperature. The trap energies were assumed to be 1.34 and 2.1 eV. According to Poon et al. [18], these trap energies were associated with single vacancies and voids. The exponential pre-factor of the trapping rate

and de-trapping rate coefficients was $2.89 \times 10^{12} \text{ s}^{-1}$ and $1.0 \times 10^{13} \text{ s}^{-1}$, respectively. In this simulation, effects of the grain boundaries were not considered by simplification. Therefore, the D diffusion in the experiments would be somewhat faster than that in the TMAP7 simulations [8].

Although no significant difference between the two simulations was observed for the cases with different trapping energies, see Fig. 5(a) and (b), D distribution in the samples was significantly different from the experimental results. It was found from the TMAP7 simulations that the trap sites were filled from the top surface. All trap sites were saturated within the fluence of less than $\sim 7.5 \times 10^{22} \text{ D}^+/\text{m}^2$, which was much lower than the experimental results. TDS measurements of hydrogen implanted by the high-energy H^- beam indicated that about 40% of irradiated H was retained in the damaged sample. It is assumed that if the trap site of hydrogen isotopes is proportional to the atomic displacements calculated by TRIM code, the H which was five times as large as the trap sites was retained around the $\sim 1 \mu\text{m}$ in depth. It can be considered that the trapping sites at the $\sim 1 \mu\text{m}$ in depth were initially filled with the high-energy implanted H. Therefore, D accumulations at the $\sim 1 \mu\text{m}$ would proceed gradually with the D fluence due to the slow isotope exchange with hydrogen.

4. Conclusion

SIMS analysis showed that D density in the damaged sample was increased with the deuterium fluences within the radiation-damaged zone. Beyond the damaged zone, D density was similar to that in the undamaged sample. Most of retained deuterium in the damaged samples was trapped in the radiation-damaged zone.

Quantitative analysis using the SIMS/NRA technique showed that D concentration at $\sim 0.1 \mu\text{m}$ in depth ($\sim 1.0 \text{ dpa}$ damage) was saturated with $\sim 0.9 \times 10^{27} \text{ D}/\text{m}^3$ at the fluence of less than $\sim 5.0 \times 10^{23} \text{ D}^+/\text{m}^2$. On the other hand, D concentration at $\sim 1.0 \mu\text{m}$ in depth was not saturated even at the fluence of $\sim 8.0 \times 10^{24} \text{ D}^+/\text{m}^2$. The TMAP7 simulations showed that the im-

planted D filled the 1.34 and 2.1 eV trap sites from the top surface and all the trap sites were filled with D at the fluence of $\sim 7.5 \times 10^{22} \text{ D}^+/\text{m}^2$, which was much lower than the experimental results. This slow increase in D density at $\sim 1.0 \mu\text{m}$ in depth could be due to slow isotope exchange with H.

TDS spectra obtained from the $\sim 4.8 \text{ dpa}$ damaged samples had three desorption peaks at $\sim 770 \text{ K}$, $\sim 860 \text{ K}$, and $\sim 920 \text{ K}$. D retention associated with the $\sim 770 \text{ K}$ peak was increased with the D^+ fluences, while that with the $\sim 860 \text{ K}$ peak was constant regardless of the D fluence. The $\sim 920 \text{ K}$ peak appeared only for the damaged samples and was also increased with the D^+ fluences. Therefore, the implanted deuterium was trapped at the radiation-induced defects associated with the $\sim 770 \text{ K}$ and $\sim 920 \text{ K}$ desorption peaks.

References

- [1] A.A. Pisarev, A.V. Varava, S.K. Zhdanov, *J. Nucl. Mater.* 220–222 (1995) 926.
- [2] R. Sakamoto, T. Muroga, N. Yoshida, *J. Nucl. Mater.* 233–237 (1996) 776.
- [3] V.Kh. Alimov, B.M.U. Scherzer, *J. Nucl. Mater.* 240 (1996) 75.
- [4] A. A. Haasz, J.W. Davis, *J. Nucl. Mater.* 241–243 (1997) 1076.
- [5] A. A. Haasz, J.W. Davis, M. Poon, R.G. Macaulay-Newcombe, *J. Nucl. Mater.* 258–263 (1998) 889.
- [6] R. Causey, K. Wilson, T. Venhaus, W.R. Wapler, *J. Nucl. Mater.* 266–269 (1999) 467.
- [7] R.A. Anderl, R.J. Pawelko, S.T. Schuetz, *J. Nucl. Mater.* 290–293 (2001) 38.
- [8] A.A. Haasz, M. Poon, R.G. Macaulay-Newcombe, J.W. Davis, *J. Nucl. Mater.* 290–293 (2001) 85.
- [9] V.Kh. Alimov, K. Ertl, J. Roth, *J. Nucl. Mater.* 290–293 (2001) 289.
- [10] O.V. Ogorodnikova, J. Roth, M. Mayer, *J. Nucl. Mater.* 313–316 (2003) 469.
- [11] B.M. Oliver, R.A. Causey, S.A. Maloy, *J. Nucl. Mater.* 329–333 (2004) 977.
- [12] I.I. Arkhipov, S.L. Kanashenko, V.M. Sharapov, R. Kh. Zalavutdinov, A.E. Gorodesly, *J. Nucl. Mater.* 363–365 (2007) 1168.
- [13] G.R. Longhurst, TMAP7: Tritium Migration Analysis Program, User Manual, Idaho National Laboratory, INEEL/EXT-04-02352, 2004.
- [14] T. Inoue, M. Taniguchi, T. Morishita, M. Dairaku, M. Hanada, T. Imai, M. Kashiwagi, K. Sakamoto, T. Seki, K. Watanabe, *Nucl. Fus.* 45 (2005) 790.
- [15] L.K. Keys, J. Moteff, *J. Nucl. Mater.* 34 (1970) 260.
- [16] Y. Ueda, T. Shimada, M. Nishikawa, *Nucl. Fus.* 44 (2004) 62.
- [17] J.F. Ziegler, J.P. Biersack, U. Littmark, *The Stopping and Range of Ions in Solids*, Pergamon, New York, 1985.
- [18] M. Poon, A.A. Haasz, J.W. Davis, *J. Nucl. Mater.* 374 (2008) 390.